

Steady Stokes Flow with Long-Range Correlations, Fractal Fourier Spectrum, and Anomalous Transport

Michael A. Zaks

Institute of Physics, Humboldt University of Berlin, 10115 Berlin, Germany

Arthur V. Straube

Physics Department, Perm State University, 614990 Perm, Russia

(Received 30 July 2002; published 20 November 2002)

We consider viscous two-dimensional steady flows of incompressible fluids past doubly periodic arrays of solid obstacles. In a class of such flows, the autocorrelations for the Lagrangian observables decay in accordance with the power law, and the Fourier spectrum is neither discrete nor absolutely continuous. We demonstrate that spreading of the droplet of tracers in such flows is anomalously fast. Since the flow is equivalent to the integrable Hamiltonian system with 1 degree of freedom, this provides an example of integrable dynamics with long-range correlations, fractal power spectrum, and anomalous transport properties.

DOI: 10.1103/PhysRevLett.89.244101

PACS numbers: 47.53.+n, 05.45.-a

The last two decades have witnessed growing interest in theoretical and applied aspects of chaotic advection in steady or temporally periodic velocity fields of hydrodynamical flows [1,2]. The contrast between the trivial behavior of the field and the complicated dynamics of individual fluid particle is due to the fact that the field is usually described by means of Eulerian variables in the laboratory reference frame, whereas for the fluid particle the Lagrangian description is more appropriate, since its reference frame is carried by the flow. An Eulerian observer performs measurements in the fixed point of the physical space and registers a steady or periodic process. For a Lagrangian observer, physical space turns into phase space, streamlines become phase trajectories, and a “measuring device” is advected along these trajectories and explores different regions of the flow pattern. Therefore the motion of the fluid particle can be chaotic in spite of the time-independent state at any given place. A consequence of this dynamics is intensive stirring and mixing. Examples of chaotic advection are widespread, from microscopical flows of nanotechnology and cellular biology to large-scale phenomena in astrophysics and geophysics; for a list of references see a recent review [3].

To exhibit Lagrangian chaos, a flow of incompressible fluid must be three dimensional, time dependent, or both. In two-dimensional setup, there is no place for exponential divergence of streamlines, and in conventional examples the motion of a typical fluid particle is periodic and well correlated. Below, we discuss a class of steady two-dimensional flows for which the correlations decay and the power spectra are fractal.

Consider a slow steady flow of a viscous incompressible fluid past the square lattice of parallel solid circular cylinders. We restrict ourselves to the “transverse” case when the component of the flow along the cylinder axes is absent. This geometry is typical, e.g., for the cooling

flows past the rods of the reactor; on the other hand, it serves as the starting point for the analysis of fluid motions in composite and porous media. Usual assumptions of the creeping flow allow one to neglect nonlinear terms in the Navier-Stokes equations and reduce them to the Stokes equations for the velocity \mathbf{V} and pressure p :

$$-\nabla p + \eta \Delta \mathbf{V} = 0, \quad \text{div} \mathbf{V} = 0, \quad (1)$$

where η is the viscosity of the fluid. Boundary conditions enforce periodicity on the borders of the elemental cell of the lattice, as well as vanishing velocity on the border $\partial\Gamma$ of the cylinder Γ . If the axes x and y are aligned along the axes of the lattice, and the cell size is chosen as the length unit, the boundary conditions are

$$\mathbf{V}(0, y) = \mathbf{V}(1, y), \quad \mathbf{V}(x, 0) = \mathbf{V}(x, 1), \quad \mathbf{V}|_{\partial\Gamma} = 0. \quad (2)$$

Formulation of the boundary problem is completed by prescribing the components of mean flow along both axes:

$$\int_0^1 V_x dy = \alpha, \quad \int_0^1 V_y dx = \beta. \quad (3)$$

Equations (1)–(3) were treated in terms of periodic Green’s function by Hasimoto who evaluated the drag on a cylinder [4]; the fundamental solution was expressed in terms of series containing elliptic functions [5]. Permeability of the array of cylinders was estimated in [6]. As every two-dimensional flow of incompressible fluid, the problem can be cast into a Hamiltonian frame by introducing the stream function $\Psi(x, y)$: $V_x = \partial\Psi/\partial y$ and $V_y = -\partial\Psi/\partial x$. Motions along the streamlines are governed by the integrable Hamiltonian system with 1 degree of freedom in which V_x and V_y are canonical variables, and Ψ plays the role of energy. In terms of Ψ Eq. (1) turns into the biharmonic equation $\Delta\Delta\Psi = 0$.

No-slip boundary conditions require $\partial\Psi/\partial x|_{\partial\Gamma} = \partial\Psi/\partial y|_{\partial\Gamma} = 0$, whereas conditions for mean flow and periodicity are ensured by putting $\Psi(x, y) = \alpha y - \beta x + \Phi(x, y)$ where Φ has period 1 in both arguments.

We solved the biharmonic equation numerically, imposing periodic boundary conditions upon a polar grid with 600×1200 nodes; for tracer dynamics, the 2nd order interpolation scheme was used. Figure 1(a) presents the flow pattern with inclination $\alpha/\beta = (\sqrt{5} - 1)/2$ and radius of the cylinder $1/6$.

Since the flow is steady, in every point of the laboratory reference frame the values of velocity and pressure are time independent. The picture looks different in a frame attached to a neutral tracer carried by the flow. We characterize it in terms of normalized autocorrelation, defined for a time-dependent observable $\xi(t)$ as

$$C(\tau) = \frac{\langle \xi(t)\xi(t + \tau) \rangle - \langle \xi(t) \rangle^2}{\langle \xi^2(t) \rangle - \langle \xi(t) \rangle^2}, \quad (4)$$

where averaging over t is performed. Since autocorrelation is the Fourier transform of the power spectrum (the Wiener-Khinchin theorem), its properties are related to the nature of the Fourier spectral measure. For periodic and quasiperiodic dynamics, $C(\tau)$ displays series of peaks with unit or asymptotically unit amplitude at arbitrarily large values of τ ; this corresponds to the discrete (pure-point) power spectrum. In case of chaotic behavior (impossible in two-dimensional dynamics) autocorrelation decays exponentially, and the power spectrum is absolutely continuous with respect to the Lebesgue measure.

Qualitative features of the autocorrelation are independent of the choice of a generic observable. We take the absolute value $|V|$ of the velocity and measure it for the fluid particle moving along the streamline of the flow. The plot of $C(\tau)$ is presented in Fig. 2(a). The largest plotted values of τ correspond to the passage through, on the average, 3×10^4 lattice cells in the y direction. We observe that autocorrelation decays, in spite of the ordered laminar structure of the flow. The decay is slower than exponential; as seen in Fig. 2(b), the highest peaks of $C(\tau)$ which form a log-periodic lattice, decrease in

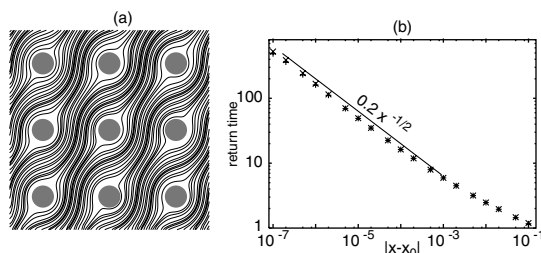


FIG. 1. (a) Flow pattern with $\alpha/\beta = (\sqrt{5} - 1)/2$; (b) divergence of passage time for streamlines near the cylinder. Crosses: numerical values; straight line: power law $\sim |x - x_0|^{-1/2}$.

accordance with the power law $C(\tau) \sim \tau^{-0.28}$. Power-law decay of autocorrelation (“long-range correlations”) is abundant in physics of critical and nearly critical states [7] and has been recovered in many natural phenomena, from DNA sequences [8–10] to atmospheric variability [11]. However, to our knowledge, such decay has been reported neither in the context of steady two-dimensional flows nor in a more general context of integrable autonomous Hamiltonian systems with 1 degree of freedom, where the correlations are usually not supposed to decay at all. Our results show that integrability does not guarantee against the decay of correlations.

Properties of autocorrelation characterize both qualitatively and quantitatively the set which supports the Fourier spectral measure. A useful tool is the integrated autocorrelation $C_{\text{int}}(t) = t^{-1} \int_0^t C(\tau)^2 d\tau$: if $C_{\text{int}}(t)$ vanishes in the limit $t \rightarrow \infty$, the power spectrum does not include the discrete component. Furthermore, $C_{\text{int}}(t) \sim t^{-D_2}$ where D_2 is the correlation dimension of the spectral measure [12]. The decay of $C_{\text{int}}(t)$ over several orders of magnitude in Fig. 2(c) indicates the absence of the discrete component in the Fourier spectrum of the tracer velocity. Estimation of the curve slope yields $D_2 \approx 0.82$; hence, the set which supports spectral measure is fractal. Apparently, in this intermediate situation between chaos and order the Fourier spectrum of velocity is singular continuous: neither discrete nor absolutely continuous.

Origin of this unconventional state can be understood if the viscous flow is viewed as a dynamical system. From this point of view, Eqs. (1)–(3) describe the area-preserving vector field $\dot{x} = V_x(x, y)$, $\dot{y} = V_y(x, y)$ on a 2-torus whose rotation number σ equals α/β . Peculiarity of this field is its identical vanishing on the cylinder border $\partial\Gamma$: no-slip boundary conditions turn each point of $\partial\Gamma$ into the fixed point. Below, we deal with irrational values of σ . Most of the existing work on dynamics on 2-tori, starting with the classical paper in

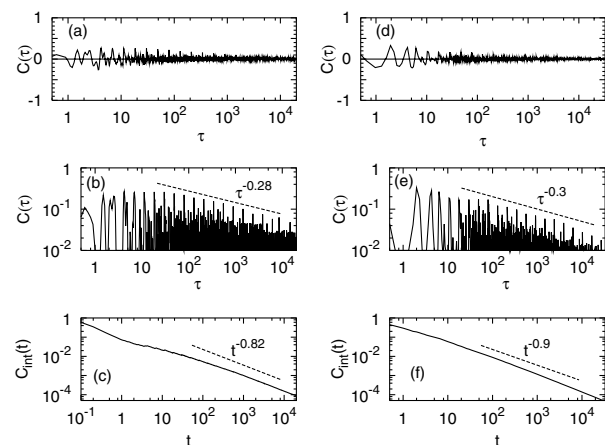


FIG. 2. Autocorrelation and integrated autocorrelation. (a)–(c) Stokes flow (1)–(3); (d)–(f) special flow (5). Dashed lines: power laws.

[13], refers to fields without fixed points. Consider a mapping of a line transversal to the flow (e.g., the boundary $y = 0$ of the square) onto itself. In the absence of fixed points, the “return time” $\tau_{\text{ret}}(x)$ needed for one iteration of this mapping (a turn around the torus) is bounded. As a consequence, dynamics of the flow is adequately reproduced by the circle map $x \rightarrow (x + \sigma) \bmod 1$. For a passive tracer in such quasiperiodic flow, the Fourier spectrum is discrete, and the autocorrelation does not decay.

The presence of stagnation points in which the velocity vanishes qualitatively changes dynamics. In this situation $\tau_{\text{ret}}(x)$ as a function of x diverges, and equivalence with the Poincaré map is invalidated: the flow with continuous power spectrum can induce the map with purely discrete spectrum [14]. Near the streamline which leads into a generic isolated stagnation point, the return time has a logarithmic singularity. Such stagnation points exist in forced viscous flows with doubly periodic arrays of steady vortices, and the Fourier spectra in these flows are fractal [15]. Logarithmic singularities of return times are too weak to make the flow mixing [16]. Stronger, powerlike singularities can produce mixing [17]; however, for isolated stagnation points such singularities occur only in degenerate, structurally unstable cases.

In the flow pattern of (1)–(3) the whole curve $\partial\Gamma$ can be viewed as a structurally stable family of stagnation points. Fluid particles exhibit the strong slowdown during their motion along the edge of the obstacle. The collective effect of this continuum of equilibria manifests itself in the power-law divergence of return time: let $(x_0, 0)$ lie on the streamline which separates the particle paths passing the obstacle “on the left” from the paths passing “on the right,” then $\tau_{\text{ret}}(x) \sim 1/\sqrt{|x - x_0|}$ [Fig. 1(b)]. The existence of this singularity ensures the decay of correlations and creates a continuous component in the power spectrum.

Let us proceed from advection of individual passive tracer to the transport of the ensemble of tracers by the flow. Figure 3 shows the temporal evolution of the initially compact droplet formed by 10^4 fluid particles. Non-

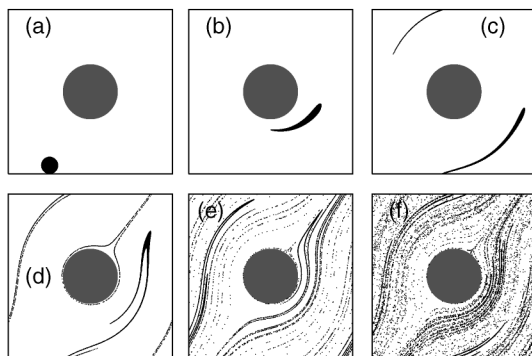


FIG. 3. Cloud of passive tracers carried by the flow. (a) $t = 0$; (b) $t = 0.5$; (c) $t = 2$; (d) $t = 5$; (e) $t = 20$; (f) $t = 100$.

isochronicity of rotations around the torus stretches the droplet. The strongest effect is observed during the passages in which the obstacle is sandwiched between the streamlines: some particles hover in the vicinity of the obstacle for the very long time, whereas the tracers which pass at a larger distance are long gone. Because of the irrational rotation number, each streamline is dense on the torus; hence, each particle passes arbitrarily close to the cylinder where its velocity becomes arbitrarily small. As a result, after a hundred passages the particles are spread over virtually the whole area of the square. Naturally, this mixing is slower and less efficient than mixing enabled by chaotic advection under Lagrangian chaos [1,2]. Nevertheless, ultimately it leads to the same result.

To quantify the rate of the spreading of the droplet on the infinite plane, we introduce the displacement $\xi_y(t) \equiv y(t) - y(0)$ and estimate the time growth of the variance $\zeta^2(t) = \langle \xi_y^2(t) \rangle - \langle \xi_y(t) \rangle^2$ by averaging over all initial positions within the unit cell. Figure 4 shows that growth of $\zeta(t)$ is described by the power law whose exponent exceeds the “normal diffusion” value $1/2$.

For larger values of t the computed values of $\zeta(t)$ undershoot the expected power law. We assign this discrepancy to insufficient statistics: slow saturation in the dependence of ζ on the length of the sample over which the averaging is made. As t grows, the main contribution into $\zeta(t)$ is made by rare “large events”: passages extremely close to the obstacle. Apparently, the longest numerically affordable to us trajectories with 3×10^6 turns around the torus ($t \approx 2.8 \times 10^6$) are still insufficient. In order to extend the range of t in which the estimates of $\zeta(t)$ are reliable, we have used the model which is computationally much less expensive: the “special flow” (flow over the mapping), often employed in ergodic theory [18]. For the map $u \rightarrow f(u)$ and the function $\tau(u)$, this dynamical system is introduced on the part of the plane u, v defined by $0 \leq v < \tau(u)$, as follows: the orbit starts at $t = 0$ in the point (u_0, v_0) , and moves with unit velocity parallel to v axis until reaching the border $\tau(u_0)$; from there it jumps to the point $(f(u), 0)$, begins the

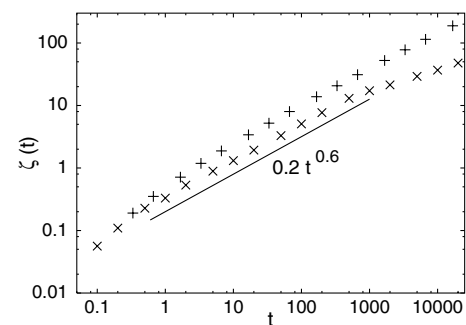


FIG. 4. Growth of variance in the ensemble of particles carried by the flow. Crosses: Stokes flow (1)–(3); pluses: special flow (5) with $C = 0.3$; straight line: $t^{0.6}$.

next stage of motion along v , and so on. Obviously, on the u axis $f(u)$ is the Poincaré mapping, and $\tau(u)$ is the return time. The trajectory is described by the expressions

$$u_t = f^n(u_0), \quad v_t = v_0 + t - \sum_{j=0}^{n-1} \tau(f^j(u_0)) \quad (5)$$

with integer $n = n(t)$ uniquely defined by inequalities

$$\sum_{j=0}^{n-1} \tau(f^j(u_0)) < v_0 + t < \sum_{j=0}^n \tau(f^j(u_0)). \quad (6)$$

The special flow for our hydrodynamical problem combines the circle map $f(u) = (u + \alpha/\beta) \bmod 1$ with the return time $\tau(u) = C/\sqrt{|u - 1/2|}$. Properties of autocorrelation for the flow (5), presented in Figs. 2(d)–2(f), are in qualitative and good quantitative accordance with the respective characteristics of the Stokes flow: autocorrelation decays as the power law, and the Fourier spectrum is fractal. To evaluate the transport in (5) we used the lift of $f(u)$ onto the real axis. Estimates obtained from 10^{10} iterations of f are shown in Fig. 4 by pluses. Again, we see the anomalously fast growth of the variance.

These unusual transport properties are related to the distribution of return times. For T large, the proportion of returns with duration between T and $T + dt$ decreases as $\sim T^{-3} dt$; the second moment of this distribution (mean square of τ_{ret}) is infinite. This is reminiscent of Lévy flights: random walks with power-law statistics and infinite moments. Widespread in physics, Lévy flights exhibit long-range correlations and anomalous transport [19,20]. Of course, the completely deterministic motion of a tracer in a flow (1) is not a random walk; the sequence of return times is rigidly prescribed by the rotation number. Nevertheless, as we see, already the presence of the power-law tail T^{-3} appears to suffice for the onset of typical hallmarks of the Lévy flights.

In dynamics of nonintegrable Hamiltonian systems, anomalous diffusion is ascribed to sticking trajectories near the Kolmogorov-Arnol'd-Moser surfaces and Cantori [21,22]. In fluid dynamics, Lévy flights were experimentally observed in time-dependent flows with coherent structures (jets, vortices, etc.), which serve as a kind of trap for tracer particles [23–25]. Our example shows that similar anomalously fast transport can take place also in the framework of the two-dimensional time-independent flow. Moreover, both basic ingredients, irrational rotation number and vanishing velocity along the whole borderline, are generic within the considered class of Stokes flows. Of course, for a “random” rotation number α/β the peaks of the autocorrelation would not form a regular lattice.

In conclusion, we have studied the spectral and transport properties of a plane steady viscous flow past an

array of solid obstacles. On reducing the problem to the time-independent integrable Hamiltonian system with 1 degree of freedom, we find fractal Fourier spectrum, long-range correlations, and anomalously fast “superdiffusive” transport reminiscent of Lévy flights.

We thank F.H. Busse, D.V. Lyubimov, A. Pikovsky, and J. Kurths for fruitful discussions and H. Hasimoto for providing the preprint [5]. The research of A.S. has been enabled by the trilateral Russian-German-French program and Grant No. PE-009-0 of CRDF, and M. Z. was supported by SFB-555.

-
- [1] H. Aref, *J. Fluid Mech.* **143**, 1 (1984).
 - [2] J.M. Ottino, *The Kinematics of Mixing: Stretching, Chaos and Transport* (Cambridge University Press, Cambridge, 1989).
 - [3] H. Aref, *Phys. Fluids* **14**, 1315 (2002).
 - [4] H. Hasimoto, *J. Fluid Mech.* **5**, 317 (1959).
 - [5] H. Hasimoto, *Lect. Notes Res. Inst. Math. Sci. Kyoto Univ.*, No. 214 (1974) (in Japanese).
 - [6] A.S. Sangani and C. Yao, *Phys. Fluids* **31**, 2435 (1988).
 - [7] H.E. Stanley *et al.*, *Physica (Amsterdam)* **200A**, 4 (1993).
 - [8] W. Li and K. Kaneko, *Europhys. Lett.* **17**, 655 (1992).
 - [9] A. Arneodo *et al.*, *Phys. Rev. Lett.* **74**, 3293 (1995).
 - [10] B. Audit *et al.*, *Phys. Rev. Lett.* **86**, 2471 (2001).
 - [11] E. Koscielny-Bunde *et al.*, *Phys. Rev. Lett.* **81**, 729 (1998).
 - [12] R. Ketzmerick, G. Petschel, and T. Geisel, *Phys. Rev. Lett.* **69**, 695 (1992).
 - [13] A.N. Kolmogorov, *Dokl. Akad. Nauk SSSR Ser. Mat.* **93**, 763 (1953).
 - [14] A.S. Pikovsky *et al.*, *Phys. Rev. E* **52**, 285 (1995).
 - [15] M.A. Zaks, A.S. Pikovsky, and J. Kurths, *Phys. Rev. Lett.* **77**, 4338 (1996).
 - [16] A.V. Kochergin, *Math. Notes* **19**, 277 (1976).
 - [17] A.V. Kochergin, *Math. Sbornik* **96**, 471 (1975).
 - [18] I.P. Cornfeld, S.V. Fomin, and Ya.G. Sinai, *Ergodic Theory* (Springer, New York, 1982).
 - [19] J.P. Bouchaud and A. Georges, *Phys. Rep.* **195**, 127 (1990).
 - [20] *Lévy Flights and Related Topics in Physics*, Lecture Notes in Physics Vol. 450, edited by M.F. Schlesinger, G.M. Zaslavsky, and U. Frisch (Springer, Berlin, Heidelberg, 1995).
 - [21] T. Geisel, A. Zacherl, and G. Radons, *Phys. Rev. Lett.* **59**, 2503 (1987).
 - [22] G.M. Zaslavsky, in Ref. [20].
 - [23] T.H. Solomon, E.R. Weeks, and H.L. Swinney, *Phys. Rev. Lett.* **71**, 3975 (1993).
 - [24] E.R. Weeks, T.H. Solomon, J.S. Urbach, and H.L. Swinney, in Ref. [20].
 - [25] S.C. Venkataramani, T.M. Antonsen, and E. Ott, *Phys. Rev. Lett.* **78**, 3864 (1997).